# Investigation of the magnetism of terbium ethylsulphate below 1 K using the Faraday effect

J. M. Daniels,* M. T. Hirvonen, A. P. Jauho, T. E. Katila, and K. J. Riski
*Department of Technical Physics, and Low Temperature Laboratory, Helsinki University of Technology, SF-02150 Otaniemi, Finland*
(Received 23 December 1974)

Plane-polarized light was passed through a single crystal of terbium ethylsulphate, parallel to the $c$ axis, at temperatures between 77 mK and 1.5 K, in magnetic fields up to 3 kG. The Faraday rotation was measured, and above the transition temperature (240 mK) was fitted to theoretical magnetization curves. Below the transition temperature, hysteresis was observed, and also depolarization of the light. The observations are consistent with a ferromagnetic state in domains parallel to the $c$ axis below the transition. Molecular-field calculations also indicate ferromagnetism. The value of the splitting between the two ground-state singlets was determined.

## I. INTRODUCTION

The subject of magnetic ordering brought about by magnetic dipole-dipole interactions is one of long-standing interest. A more recent topic is that of spontaneously ordered states in systems which have a singlet ground state. That such ordered states might exist was suggested by Trammell[1] and elaborated by others,[2] but the attention of these authors has been directed mainly towards exchange as a source of magnetic coupling rather than towards magnetic dipole-dipole interaction. Terbium ethylsulphate is probably for several reasons an ideal substance in which to study singlet-state magnetic ordering produced by magnetic dipole interaction. First of all, the $g$ value of the $Tb^{+++}$ ion is large, 17.8, and hence the interactions are strong; also the ion is easily polarized because the first excited state is only about 1 K above the ground state. Second, the ethylsulphates of the rare earths are a well-studied series, and there is abundant evidence that there is no exchange coupling between rare-earth ions in these salts. This has been demonstrated in particular for $Tb^{+++}$.[3] A suggestion has been made many times that the magnetism of rare-earth ethylsulphates may be easily explained theoretically on account of a similarity between these substances and the Ising model.[4] Be that as it may, studies have recently been made of terbium ethylsulphate; for example, the specific heat has been measured, an anomaly indicating the onset of magnetic order has been found at 240 mK, and measurements of the magnetic susceptibility have also indicated a magnetic transition at the same temperature.[5] However, as these authors point out, their method does not easily distinguish unambiguously between a ferromagnetic state and other magnetic states, because the method is not very sensitive to changes in susceptibility when the susceptibility is large, and because the expected variation of susceptibility with temperature in the ferromagnetic state is model dependent and not precisely known. The problem was therefore to determine experimentally whether the ordered state of terbium ethylsulphate is ferromagnetic or some other state.

The Faraday effect has often been used to measure magnetization. It is particularly suitable for rare-earth compounds because their Faraday rotations are quite large. We expected that it would also show distinction between antiferromagnetism and ferromagnetism in long thin domains with opposite magnetization. In the former case, the Faraday rotation ought to be zero, because the average magnetization is zero, and there would be both up and down spins separated by only a few angstroms, a distance much less than the wavelength of the light used and therefore unresolvable. In the latter case, it is known that, if the domains are big enough, it is possible to see them by the opposite rotations of the plane of polarization of light with different senses of magnetization. If the domains are too small to be resolved, some other distinctive feature ought to be noticed.[6]

We therefore thought it appropriate to observe terbium ethylsulphate below its transition temperature by using the Faraday effect. The temperatures needed are very low, requiring a dilution refrigerator to produce them, and this introduces difficulties of an experimental nature. We have carried out such an experiment successfully, and this is reported in the following sections.

## II. SPECIMEN AND APPARATUS

The specimen was made starting from 99.9% terbium oxide, $Tb_4O_7$.[7] The material was checked by EPR, optical spectroscopy, and neutron activation analysis, and only negligible amounts of other rare earths were detected.

The oxide was first dissolved in reagent-grade hydrochloric acid, then the sulphate was precipitated with excess of reagent-grade sulphuric acid and recrystallized from water. Barium ethylsulphate was prepared by refluxing ethyl alcohol with sulphuric acid on a water bath, followed by neutralization with barium carbonate. Stoichiometric quantities of barium ethylsulphate, previously purified by being twice recrystallized from water at room temperature under reduced pressure, and terbium sulphate, in aqueous solution, were mixed to give a solution of terbium ethylsulphate. The clear solution was filtered and evaporated under reduced pressure, and the material thus obtained was purified by a further recrystallization.

The crystals used in this experiment were grown from a saturated solution containing about 30 g of terbium ethylsulphate, in a desiccator at atmospheric pressure, in a constant temperature room. The seed crystals were glued on to a paddle which was rotated back and forth in the solution, and the growing crystal was never allowed to get dry; in this way it was possible to obtain terbium ethylsulphate crystals of reasonable optical quality, free from veils and inclusions, about $\frac{1}{2}$–1 cm in linear dimension. A plate was cut from one of these crystals, the plane of which was perpendicular to the hexagonal axis. It was thinned down and polished by being rubbed gently on moist filter paper. The final specimen was $0.57_2$ mm thick and somewhat irregular in outline, being about 8 mm across; when considering its magnetic properties, we assumed it to be an oblate spheroid of axial ratio 1:14, for which the demagnetizing factor is $0.9 \times 4\pi$.

The terbium ethylsulphate specimen was cooled to temperatures in the range of 0.07–1.5 K inside the mixing chamber of a $^3$He-$^4$He dilution refrigerator. This refrigerator, which was originally designed for Mössbauer experiments, has been described elsewhere.[8] In the final versions of the experiment, the following changes were made (see Fig. 1).

The Mössbauer drive was removed, leaving a vertical hole 1 cm in diameter from the top of the cryostat to the mixing chamber. The top of the cryostat was sealed with a Perspex plate pressed on to a rubber O ring. The light source was the quartz inner element of a high-pressure mercury lamp used for street lighting[9]; it was mounted inside a water-cooled tube. A parallel beam of light was obtained using a collimator consisting of a pinhole in a copper foil, a gelatine filter, and an interference filter which together passed the 5460-Å green mercury light, and a 15 cm focal length lens. This combination of lamp and collimator was mounted above the Perspex window so as to direct a parallel beam of light vertically downwards on to the mixing chamber. A piece of heat-absorbing glass (the kind used in slide projectors) was placed in the beam and anchored thermally to the liquid-helium bath. Next was a piece of polaroid sheet, mounted on a metal frame about 3 cm above the top of the mixing chamber, and supported from the pillars from which the various parts of the dilution refrigerator are suspended.

The mixing chamber was fitted with Pyrex windows which were clamped down on to the body of the mixing chamber with metal rings and sealed with indium O rings. The specimen was stuck to the bottom of the upper window with a thin layer of silicone vacuum grease, and further held in position with a cotton thread stretched across it. The mixing chamber also contained a carbon re-

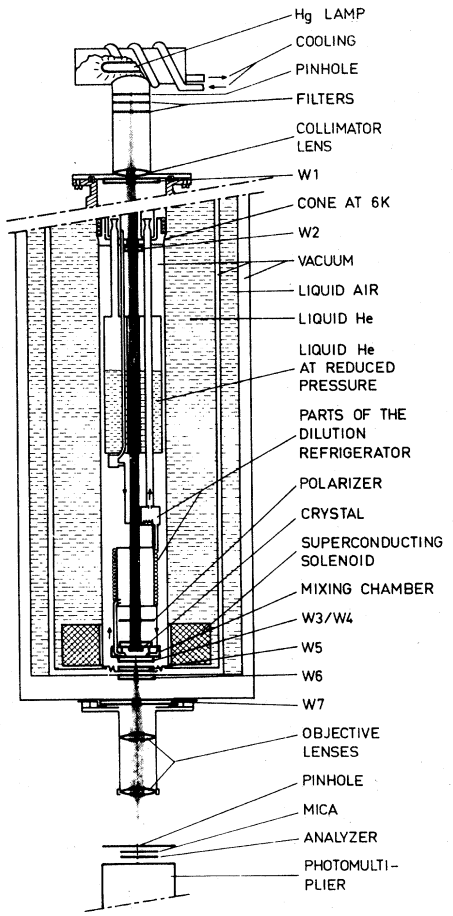


FIG. 1. Schematic diagram of the measurement setup. The figure shows the path of light from the lamp to the detector (*W*, window). Also shown are parts of the refrigeration system. The crystal to be measured is located inside the mixing chamber of the dilution refrigerator.

sistance thermometer and a germanium resistance thermometer; these thermometers were calibrated against cerium magnesium nitrate in a separate experiment.

The original three beryllium windows in the bottom of the helium Dewar were replaced with glass ones. The one at liquid-helium temperature was a Pyrex window stuck onto a thin corrugated copper plate with epoxy.[10] The window in the radiation shield was made of heat-absorbing glass, and the one at room temperature was also of Pyrex, sealed with a rubber O ring. All the windows below the polarizer were annealed to relieve strains, and all optical parts below the terbium ethylsulphate crystal were given antireflection coatings on all surfaces.

Two optical systems were used to examine the light passing through the bottom window. In the first experiments, a microscope, made up of two 15-cm focal-length objective lenses and a 1-cm focal-length eyepiece, permitted direct visual observation of the crystal. The eyepiece, which contained a polaroid, could be rotated, and its position could be read off on a scale engraved round the microscope tube.

In later experiments a polarimeter was used to make a complete analysis of the state of polarization of the light. For this, the eyepiece was removed to project an image of the crystal about $2\times$ magnified on to a white cardboard screen. About 5 min of dark adaption were needed to enable an experimeter to see this image clearly. The screen had a 3-mm-diameter hole and could be positioned to pass light from any desired part of the image through the polarimeter onto a photomultiplier.[11] The mercury lamp was lit from the 50-Hz mains, and thus the light was modulated at 100 Hz. The output of the photomultiplier was fed into a phase sensitive detector, the reference being 100 Hz obtained from the mains using a full-wave rectifier. The output from the phase-sensitive detector was displayed on a digital voltmeter. The linearity of the system was verified using the well-known $\cos^2\theta$ law for the intensity of light passed by two polaroids.

The polarimeter consisted of two elements; the light first passed through a mica plate whose retardation was approximately a quarter wavelength, and then it passed through a polaroid. The mica plate could be rotated about a vertical axis with stops situated so that its fast direction could be easily placed at $\pm 27.5^\circ$ from the zero of azimuth (an arbitrary zero which was lined up as close as possible to the plane of polarization of the light in the incident beam). Similarly, the polaroid could be rotated about the same axis, so that its plane of polarization could also be easily placed at $\pm 27.5^\circ$ from the same zero. The polarization state of the light incident on the polarimeter was determined by measuring the intensity of light passed for all four combinations of position of both the mica and the polaroid. Details of how these four readings are converted into more conventional parameters are given in the Appendix.

## III. MEASUREMENTS

Light in any arbitrary state of polarization can be regarded as a mixture of unpolarized light and elliptically polarized light. The elliptical polarization can be further characterized by the angle $\alpha$ which the major axis makes with the zero of azimuth, and the angle $\beta$ of "opening" of the ellipse defined by $\tan\beta = b/a$, where $a$ and $b$ are, respectively, the major and minor axes of the ellipse (see Fig. 8). Thus there are three parameters which characterize the state of polarization of the light, the intensity fraction of unpolarized light, and the angles $\alpha$ and $\beta$. This representation is only one of many possible descriptions of the state of polarization; we chose to use it because of the simplicity of interpretation of our measurements when presented in this form.

In every one of our measurements, the angle $\beta$ was of the order of $1^\circ$ in magnitude. We can therefore consider $\beta = 0$ within the limits of experimental error, and the emergent light consisted of a mixture of unpolarized light and plane polarized light. Although the crystal appeared to be of good optical quality to the eye, it was not so good when examined by the polarimeter. At all temperatures from room temperature to 240 mK the emerging light contained about 20% of unpolarized light. Further, the crystal looked a bit spotty when examined with polarized light and a polarizing eyepiece. However, above 240 mK it was possible, by using the polarizing eyepiece, to extinguish the light passing through the crystal, with the exception of a few bright "dots." Apparently, the background of 20% of unpolarized light was caused by these defects in the crystal.

Magnetization curves were made above 240 mK, using the field produced by a superconducting solenoid. As the specimen was magnetized, the rotation of the plane of polarization increased, and the intensity fraction of unpolarized light remained constant at about 20%. One such magnetization curve is shown in Fig. 2., where a calculated curve is also shown.

The spin-Hamiltonian of terbium ethylsulphate is

$$\mathcal{H} = g\mu_B H_z S_z + \Delta S_x + A S_z I_z \,, \tag{1}$$

where the effective electron spin $S = \frac{1}{2}$, $I = \frac{3}{2}$, and

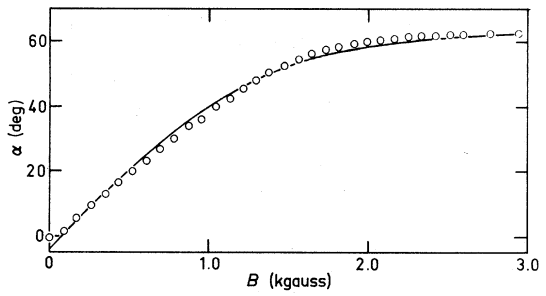


FIG. 2. An example of a magnetization curve in the paramagnetic phase. The Faraday rotation $\alpha$ is plotted against field. The temperature was 540 mK. The fitted curve has $\Delta = 0.86$ K and is the best fit with an assumed demagnetizing factor of $0.9 \times 4\pi$.

the $z$ axis is the hexagonal crystal axis. We took the values $g = 17.82 \pm 0.05$ and $A = 0.209 \pm 0.002$ cm$^{-1}$ measured by electron spin resonance on the concentrated salt.[12] In the published literature there are no values of $\Delta$, the splitting between the ground level and the first excited level, reported for the concentrated salt. A value of 0.387 cm$^{-1}$ for the dilute salt has been reported.[13] A value of $\Delta = 0.63$ K for the concentrated salt has been obtained from an analysis of the specific heat.[5] We undertook to derive a value of $\Delta$ from our magnetization measurements.

The spin Hamiltonian is easily diagonalized; it is seen that $m = I_z$ is a good quantum number and that the nucleus in a state $|m\rangle$ is equivalent to an external magnetic field $mH_n$, where $H_n = 252$ G. The energy levels are then

$$E_{\pm}(m) = \pm \tfrac{1}{2}[g^2\mu_B^2(H + mH_n)^2 + \Delta^2]^{1/2}, \tag{2}$$

and the magnetic moment of that level is

$$\mu_{\pm}(m) = \mp \frac{g\mu_B}{2} \frac{g\mu_B(H + mH_n)}{[g^2\mu_B^2(H + mH_n)^2 + \Delta^2]^{1/2}}. \tag{3}$$

The magnetization $M$ of the specimen is then given by

$$\frac{M}{M_0} = \frac{2}{g\mu_B} \sum_{m\pm} \mu_{\pm}(m) e^{-E_{\pm}(m)/kT} \Big/ \sum_{m\pm} e^{-E_{\pm}(m)/kT}. \tag{4}$$

In Eq. (4), $H$ is the field at the site of the $Tb^{+++}$ ions. The relation between $H$ and the external field $H_0$, according to molecular field theory, is

$$H = H_0 + \left[\frac{g\mu_B}{2} \sum \frac{3z^2 - r^2}{r^5} + \frac{M_0}{V}\left(\frac{4\pi}{3} - D\right)\right] \frac{M}{M_0}. \tag{5}$$

In Eqs. (4) and (5), $M_0$ is the saturation magnetization $Ng\mu_B/2$, $V$ is the gram ionic volume, $D$ is the demagnetizing factor, and the sum is a lattice sum worked out for all the ions inside a large sphere. For our specimen, the term in square brackets has a value of $-398$ G. Equations (4) and (5) together give the magnetization $M/M_0$, which is proportional to the Faraday rotation $\alpha$. This function was fitted by the method of least squares, the adjustable parameters being $\Delta$, the rotation $\alpha_0$ when $M = M_0$, and the zero of $\alpha$. The results are given in Table I.

The spread in all these values is greater than the standard deviation indicated by the statistical procedure used to calculate them. This is probably due to some systematic uncertainties which we have not been able to take into account. An example of one such source of error is the assumption that the specimen is a 14:1 oblate spheroid. Such sources of error are difficult to eliminate; we therefore estimate our errors from the actual scatter of the measured quantities. We thus find that $\Delta = 0.9 \pm 0.2$ K. The Faraday rotation at saturation is $1150 \pm 50$ deg cm$^{-1}$, and its direction is that of a left-handed helix when the light travels in the same direction as the magnetic field.

Below the transition temperature, the following behavior was observed. When the temperature is lowered in zero external field, the fraction of unpolarized light stays constant at about 20% and the Faraday rotation $\alpha$ remains zero. Then, when a magnetic field is applied, the Faraday rotation increases, and the fraction of unpolarized light increases at first, decreasing back to the usual 20% as saturation is approached. If the field is now reduced to zero, the Faraday rotation decreases almost to zero, and the fraction of unpolarized light increases to a maximum near zero field. Then, when the field is increased in a reverse direction, the Faraday rotation increases again in a reverse direction, and the fraction of unpolarized light decreases again to 20% as saturation with negative field is approached. The same behavior is observed as the field is again reversed. Hysteresis is seen both in the Faraday rotation and in the fraction of unpolarized light. This behavior is shown in Fig. 3. The amount of unpolarized light produced by magnetizing the specimen to saturation, and then reducing the field to zero, depends on the temperature, being larger at lower temperatures. (We have seen as much as 60% unpolarized light.) If the specimen is first magnetized and the field is then reduced to zero to produce a state in which a large amount of unpolarized light is seen, and then the temperature is allowed to rise, the fraction of unpolarized light stays constant until just below the transition temperature, when it begins to decrease, reaching the expected 20% at the transition temperature. One such warming curve is shown in Fig. 4.

TABLE I. Parameters resulting from the least-squares fitting of the theoretical magnetization curve in the paramagnetic phase. (Runs 1 and 2 were made on a different date from the rest.)

| Run | Temperature (K) | Δ (K) | $\alpha_0$ (deg) | $\sum$ (residuals)$^2$ | No. of points |
|---|---|---|---|---|---|
| | Assumed value of $D=0.8\times4\pi$ | | | | |
| 1 | 0.260 | 1.604±0.054 | 93.381±1.424 | 48.97 | 12 |
| 2 | 0.280 | 1.313±0.043 | 84.329±1.142 | 66.65 | 10 |
| 3 | 1.550 | 1.782±0.103 | 65.921±0.618 | 17.79 | 33 |
| 4 | 0.760 | 1.007±0.064 | 67.538±0.700 | 38.70 | 25 |
| 5 | 0.540 | 1.129±0.029 | 71.191±0.556 | 129.29 | 40 |
| Weighted average | | 1.34 | 70.2 | | |
| Weighted average of runs 3, 4, and 5 | | 1.29 | 67.2 | | |
| | Assumed value of $D=0.9\times4\pi$ | | | | |
| 1 | 0.260 | 1.331±0.050 | 90.210±1.357 | 42.83 | 12 |
| 2 | 0.280 | 1.046±0.040 | 81.669±1.106 | 52.84 | 10 |
| 3 | 1.550 | 1.389±0.126 | 64.842±0.611 | 11.57 | 33 |
| 4 | 0.760 | 0.543±0.083 | 66.018±0.684 | 22.46 | 25 |
| 5 | 0.540 | 0.858±0.031 | 69.451±0.543 | 79.64 | 40 |
| Weighted average | | 1.01 | 68.6 | | |
| Weighted average of runs 3, 4, and 5 | | 0.93 | 66.2 | | |
| | Assumed value of $D=4\pi$ | | | | |
| 1 | 0.260 | 1.039±0.046 | 86.390±1.289 | 34.70 | 12 |
| 2 | 0.280 | 0.748±0.041 | 78.468±1.074 | 35.97 | 10 |
| 3 | 1.550 | 0.866±0.210 | 63.678±0.608 | 6.80 | 33 |
| 4 | 0.760 | 0.085±0.137 | 64.543±0.668 | 17.63 | 25 |
| 5 | 0.540 | 0.513±0.041 | 67.495±0.530 | 36.43 | 40 |
| Weighted average | | 0.65 | 66.9 | | |
| Weighted average of runs 3, 4, and 5 | | 0.51 | 64.9 | | |

The behavior just described is consistent with the picture of ferromagnetism in long thin domains parallel to the hexagonal crystal axis. Because of crystal imperfections, the domain walls cannot be expected to be strictly parallel to the axis. The light, too, is not all parallel, and may also not be strictly parallel to this axis. As a result, a ray of light will traverse several domains, its plane of polarization being rotated forwards in some and backwards in others. When the average magnetization is zero, the average rotation will be zero, but there will be some spread. The larger the domains, the greater will be this spread. If such a spread is symmetrical, and it may be expected to be so since it is produced by many effects acting at random, the effect is to introduce an unpolarized component into the light. The rotation $\alpha$ is, however, the same as would be expected if there were no spread. We note the disappearance of domains when the magnetization is saturated, and when the temperature is raised above the transition point. In addition, the domain structure appears to be coarser at lower temperatures, where there is insufficient thermal agitation to facilitate the motion of domain walls.

We can test the assumption that the ordered state is ferromagnetic in long thin domains by calculating the initial magnetization curve. Suppose that the magnetization in the "up" domains (those for which the magnetization is in the direction of the external field $H_0$) is $M_+$, and in the "down" domains is $M_-$. Then the field acting on any individual spin is the sum of the external field $H_0$, a local interaction field which can be written $\lambda M_\pm$ and which is proportional to the domain magnetization, and a demagnetizing field which is proportional to the magnetic moment $M$ of the specimen as a whole. In addition, the magnetization of any individual

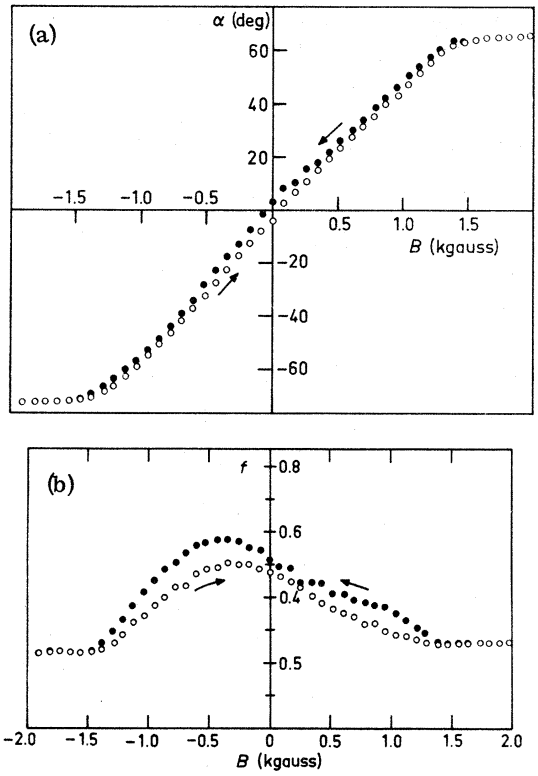


FIG. 3. (Above) Hysteresis in the rotation of the plane of polarization, and (below) hysteresis in $f$, the fraction of unpolarized light, in one cycle of magnetization at $T = 77$ mK. The bulge as $H$ approaches 0 may be due to a momentary cooling by adiabatic demagnetization.

spin depends on the field acting on it through Eq. (4); this may be written $H_\pm = f(M_\pm)$. Thus we have

$$H_\pm = f(M_\pm) = \pm H_0 + \lambda M_\pm \mp D'M\,, \tag{6}$$

where, from Eq. (5),

$$\lambda = \frac{1}{N}\sum \frac{3z^2 - r^2}{r^5} + \frac{4\pi}{3V} \quad \text{and} \quad D' = D/V\,.$$

Then, adding

$$f(M_+) - \lambda M_+ + f(M_-) - \lambda M_- = 0 \tag{7}$$

and subtracting

$$f(M_+) - f(M_-) = 2H_0 + \lambda M_+ - \lambda M_- - 2D'M\,.$$

Now, if the sizes of the domains change, so does $M$, and there are corresponding changes in $M_+$ and $M_-$. From the mathematical point of view, $M$ can be considered an independent variable, which induces corresponding changes in $M_+$ and $M_-$. At constant $H_0$, then,

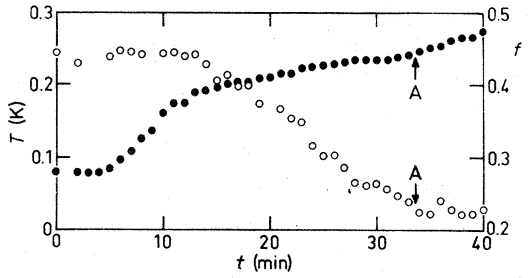


FIG. 4. Temperature $T$ (full circles), and the fraction of unpolarized light $f$ (open circles), as a function of time during warming in zero field. $A$ denotes the point of crossing the transition.

$$[f'(M_+) - \lambda]\delta M_+ + [f'(M_-) - \lambda]\delta M_- = 0$$

and

$$[f'(M_+) - \lambda]\delta M_+ - [f'(M_-) - \lambda]\delta M_- = 2D'\delta M\,.$$

Now the equilibrium state is that in which the variation $H_0\delta M$ in magnetic enthalpy is zero. Thus $\delta M = 0$, and hence

$$f'(M_-) - \lambda = 0. \tag{8}$$

This gives the magnetization $M_-$ of the "down" domains. The magnetization $M_+$ of the "up" domains is given by Eq. (7). We note that, for this value of $M_+$, $f'(M_+) - \lambda \neq 0$, but $dM_+/dM = 0$. This solution of Eq. (7) and (8) is shown graphically in Fig. 5. Putting $\lambda M_- - f(M_-) = H_e$ we have, from Eq. (6),

$$M = (H_0 - H_e)/D'\,. \tag{9}$$

The initial magnetization curve therefore consists of three parts: First, as $H_0$ is increased from 0 to $H_e$, the total magnetization remains zero, but the magnetizations of the up and down domains change. When $H = H_e$, their values are as given by Eqs. (7) and (8). For values of $H > H_e$, the mag-

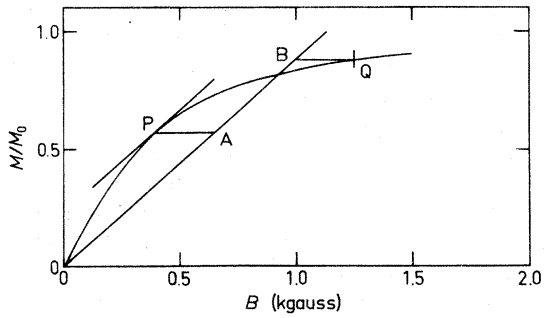


FIG. 5. Construction for finding the parameters of the initial magnetization curve in the ferromagnetic state. In this example, the curve is the ionic magnetization curve for $\Delta = 1.01$ K and $T = 77$ mK. $H_e = PA = BQ = 260$ G. Q gives $M_+ = 0.88\ M_0$. P gives $M_- = 0.57\ M_0$.

netization increases linearly with $H$, as shown by Eq. (9), until there are no down domains left. Then it should follow the paramagnetic magnetization curve as given by Eqs. (4) and (5). Figure 6 shows measurements of an initial magnetization curve, and two curves calculated according to Eq. (9). We see that the measured curve agrees well with one of the calculated curves. Using the procedure shown in Fig. 5, we find that the intercept $H_e$ depends on $\Delta$, the only disposable variable, varying approximately linearly from a value of 550 G when $\Delta = 0.5$ K to 100 G when $\Delta = 1.25$ K. The slope of the linear portion of the magnetization curve depends only on the demagnetizing factor. For the particular combination which fits the measurements well ($\Delta = 1.29$ K and $D = 0.8 \times 4\pi$), the value of $\Delta$ is that which results from a least-squares fit to the paramagnetic magnetization measurements with $D$ assumed to be $0.8 \times 4\pi$ (see Table I).

Now, a demagnetizing factor of $0.8 \times 4\pi$ corresponds to an oblate spheroid with a 6:1 axial ratio. If we use this value in Eq. (5) to calculate the magnetization curve in the paramagnetic phase, we find that the fit is noticeably worse than if the value $0.9 \times 4\pi$ is used. (We have also carried out the fitting procedure using the value $4\pi$ appropriate to a flat plate, and find rather better fits than in the other cases, as shown in Table I.) Our specimen was a flat plate of finite size—this was not only for convenience in making the specimen, but also to provide a constant optical path—and hence does not have a definite demagnetizing factor. To consider the specimen a 14:1 oblate spheroid is only an approximation. The demagnetizing field is greater near the centre and near the faces, and smaller near the edges. Although the fitting of theoretical expressions to the magnetization curves in both the ferromagnetic and paramagnetic regions is not altogether satisfactory, it is easier to justify *a priori* that the specimen should be approximated by a 14:1 oblate spheroid in these calculations, which is what we have done.

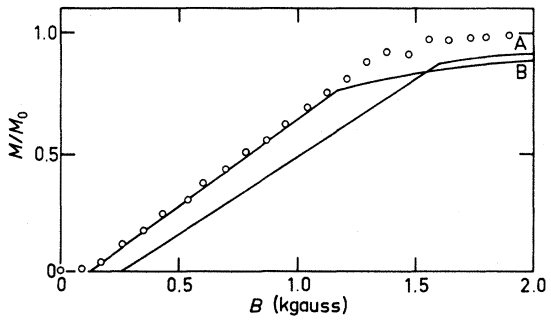


FIG. 6. The initial magnetization curve at 77 mK. Two calculated curves are shown; A is for $\Delta = 1.01$ K, $D = 0.9 \times 4\pi$; B is for $\Delta = 1.29$ K, $D = 0.8 \times 4\pi$.

## IV. MOLECULAR-FIELD PREDICTIONS

The experimental evidence presented above is quite consistent with the existence of an ordered state which is ferromagnetic in long thin domains. We might ask whether, in fact, theory predicts such a state. We have made a calculation using the simplest such theory, molecular field theory, and we find it does indeed predict a ferromagnetic ordered state.

Terbium ethylsulphate crystallizes in the hexagonal system with the same structure as that of all the other rare-earth ethylsulphates. The structure of eight members of this isomorphic series has been determined by Ketelaar.[14] There are two $Tb^{+++}$ ions in the unit cell, and their positions are shown in Fig. 7; the cell dimensions are $a = 14.05$ Å, $c = 7.11$ Å. $Tb^{+++}$ is a singlet ground-state ion for which the magnetic moment $\mu$ lies along the hexagonal ($c$ or $z$) axis, and is polarizable only by the $z$ component of the magnetic field acting on it, whose value is $H_z = \sum_i \mu_i (3z_i^2 - r_i^2)/r_i^5$. Also a self-consistency condition must be satisfied, that the field and the moment at each ionic site are related through Eq. (3).

By far the largest single contribution comes from the nearest neighbors along the $c$ axis. The field produced by each of these is $15.4\ \mu/a^3$. The total field produced by the whole of such a chain assuming equal and parallel moments on each ion is $37.0\ \mu/a^3$. The next largest contribution comes from the nearest neighbors not on the $c$ axis. Each produces a field of $-2.07\ \mu/a^3$, a total of $-12.42\ \mu/a^3$. If, however, we assume that all the spins in these chains are parallel, the field produced by one such

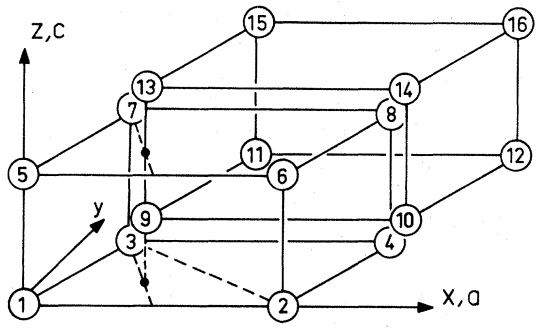


FIG. 7. Positions of $Tb^{3+}$ ions in terbium ethylsulphate. The cell is hexagonal, and the angle 3-1-2 is 60°. The ions labeled 1–8 outline a chemical unit cell. The ions labeled 1–16 show the positions of all the different ions in an $n = 2$ superlattice.

chain is $+0.632\ \mu/a^3$: It thus appears on a casual inspection that (i) the spins in each chain are all parallel, and (ii) considering the interaction between chains, the spins in different chains are parallel, thereby leading to ferromagnetism.

Such an argument was used by Cooke *et al.*[4] to predict a ferromagnetic ordered state for dysprosium ethylsulphate, a substance which, like terbium ethylsulphate, has no magnetic moment perpendicular to the $c$ axis. This argument, however, implies long thin domains, and, as presented, requires further justification. The reason is that the sum $\sum(3z^2-r^2)/r^5$ is conditionally convergent, and the value obtained depends on either the shape of the boundary (in the case of a finite sum) or the order in which the summation is carried out (in the case of an infinite sum). The case of terbium ethylsulphate also differs from that of dysprosium ethylsulphate because the condition in the latter case of constant total moment at each ion is replaced in the former by a much more complicated self-consistency condition, that the field at each ionic site should be just what is needed to produce the moment actually existing at that site.

We used a modification of the method first used by Luttinger and Tisza.[15] We assume that conditions in the ordered state repeat after two primitive lattice translations; this means a superlattice, whose cell dimensions are twice those of the crystallographic cell, and which therefore contains 16 different ions. These are shown numbered in Fig. 7. The state of magnetic ordering can be described by a 16-element vector $\vec{v}$ whose elements are the magnitude of the moment on each of the 16 sublattices. The magnetic field at each of the lattice sites can be represented by a 16-element vector $\vec{h}$, whose elements are the $z$ component of the field at each of the 16 sublattices. Then $\vec{h}$ is related to $\vec{v}$ by $\vec{h}=\underline{A}\cdot\vec{v}$, where $\underline{A}$ is a $16\times16$ matrix whose element $A_{ij}=\sum_k(3z_{ik}^2-r_{ik}^2)/r_{ik}^5$, where $r_{ik}$ and $z_{ik}$ are, respectively, the distance and the difference in $z$ coordinate between a typical ion $X$ in lattice $i$ and another in lattice $j$. The sum is taken over all the ions in lattice $j$ lying inside a large sphere whose centre lies at the ion $X$. Because of symmetry, only six of these sums are independent, and these are given in Table II.

In the case of Kramers ions the next step arises from the fact that the magnetic energy is $-\frac{1}{2}\vec{v}\cdot\underline{A}\cdot\vec{v}$. In the case of anisotropic ions this can be written $-\frac{1}{2}\vec{s}\cdot\underline{g}\cdot\underline{A}\cdot\underline{g}\cdot\vec{s}$, where $\vec{s}$ is a "classical" unit vector on each site and $\underline{g}$ is the (generalized) $g$ tensor. The matrix $\underline{g}\cdot\underline{A}\cdot\underline{g}$ is then diagonalized to give the stationary energy values, and these correspond to possible spin configurations if they also satisfy the so-called "strong condition"—that the value of $|s|^2$ on each site is the same—a condition which is almost always satisfied. The condition which has to be satisfied for non-Kramers ions is the more stringent self-consistency condition. We have followed the same procedure as that used by Gavignet-Tillard *et al.*[16] in their treatment of terbium aluminum garnet—that is, we have solved the corresponding Kramers problem and verified that, for each of the configurations which arise from this problem, the moments and the local fields at each site are all equal in magnitude (though not in sign). Hence it is possible to satisfy the self-consistency condition at all the sites simultaneously. The preferred configuration is that for which the constant of proportionality $\lambda$ between field and moment is the largest. These are listed in Table III. It is to be noted that, since the lattice sums have been evaluated inside a sphere, there is a demagnetizing field in the ferromagnetic configuration. If the specimen breaks up into long thin domains, this demagnetizing field is absent. In this case, $\lambda$ must be increased by $4\pi/3v$, where $v$ is the volume of crystal per ion; this correction is also shown in Table III. From this calculation we obtain the numerical relation used in Eqs. (5) and (6), that the interaction field

$$\left(\frac{g\mu_B}{2}\sum\frac{3z^2-r^2}{r^5}+\frac{4\pi M_0}{3V}\right)\frac{M}{M_0}=1140\,\frac{M}{M_0}\ \text{G}.$$

As is well known, an ordered state is possible for non-Kramers ions if the interaction is greater than a certain critical value. On this model, with hyperfine interaction, an ordered state is possible for any value of $\lambda>0$, because hyperfine interaction introduces a discontinuity in the magnetization curve at $H=0$ when $T=0$. We see from Table III that the ferromagnetic configuration is the energetically favored one, and that there are several antiferromagnetic configurations close in energy which would be favored before the ferromagnetic configuration, if it did not break up into domains. This calculation is essentially the same as one carried out by Langendijk *et al.*[17] for dysprosium

TABLE II. Values of $\sum(3z^2-r^2)/r^5$, in units of Å$^{-3}$, from the origin of coordinates on ion No. 1 in Fig. 7 to all ions in lattice $j$ lying within a sphere of radius 300 Å.

| $j$ | $\sum\frac{3z^2-r^2}{r^5}$ |
|---|---|
| 1 | $+0.12403\times10^{-2}$ |
| 2 | $-0.54201\times10^{-3}$ |
| 5 | $+0.11273\times10^{-1}$ |
| 6 | $-0.32103\times10^{-3}$ |
| 9 | $-0.35288\times10^{-3}$ |
| 12 | $-0.43255\times10^{-3}$ |

ethylsulphate: Unfortunately, we did not find sufficient numerical detail in their publication to enable us to use their results.

Of course, we have not proved that the ordered configuration which actually occurs in the one which comes out of this calculation. Diagonalizing the matrix $\underline{g} \cdot \underline{A} \cdot \underline{g}$ gives a set of configurations which satisfy the "weak" constraint, and which, if they also satisfy the "strong" constraint, are, for Kramers ions, (i) configurations of stationary energy, (ii) the only configurations of stationary energy, and (iii) configurations that contain the configuration of absolutely lowest energy for that particular superlattice. If the procedure is repeated for different superlattices (repetition after $n$ lattice spacings, where $n = 2, 3, 4$, etc.) it is possible to pick out the configuration of lowest energy, although this involves an enormous amount of labour. The procedure also gives configurations which transform like basis functions for irreducible representations of the lattice translation group, which makes it easy to spot them by inspection.

Now these configurations have the property that the magnetic field at each site is proportional to the moment at that site, and since the self-consistency condition is nonlinear, it cannot in general be satisfied simultaneously at all the sites. It is satisfied simultaneously for some of these configurations, for example, those which arise from $n = 2$ (where all the fields and moments are equal in magnitude, though different in sign), from $n = 4$ (where the sequences of moments may be $+\mu, 0, -\mu, 0, \ldots$ or $+\mu, +\mu, -\mu, -\mu$) and for some of the configurations which arise from $n = 3$ [for example the $\sin(2\pi l/3)$ configuration for which the moments follow the sequence $0, +\mu, -\mu, \ldots$, but not in general for the $\cos(2\pi l/3)$ configuration for which the moments follow the sequence $+\mu, -\mu/2, -\mu/2$]. It can, however, be satisfied for configurations which are not eigenfunctions of $\underline{g} \cdot \underline{A} \cdot \underline{g}$. For example, for two sublattices, a "modulated ferromagnetic" configuration (i.e., one in which the moments are all positive and alternate in magnitude) is possible, and can be energetically favored over the ordinary ferromagnetic configuration. Whether this actually occurs or not depends on the precise values of the interaction parameters and on the form of the relation between field and moment. Bidaux *et al.*[18] have developed a method of solving and visualizing the self-consistent states of a two-sublattice non-Kramers ordered state, but they do not appear to have explored all the possibilities of their method, and it is difficult to see how it could be extended to configurations with more than two sublattices. We can, however, find some of these configurations in the following way. For a modulated ferromagnetic configuration, let us write the moments on the two lattice sites as $\mu_1 = m + s$ and $\mu_2 = m - s$. Then the fields at these lattice sites are given by equations of the form $H_1 = am + bs$, $H_2 = am - bs$. It is easy to see that, provided $a$ and $b$ are both positive and large enough, and $b > a$, configurations exist which satisfy the self-consistency condition. It is easy to see, also, that this treatment will find self-consistent configurations which are a combination of two simple antiferromagnetic configurations, and, also, that all these configurations are higher in energy than the simple ones out of which they are constructed.

We should, therefore, regard the procedure of adapting the Kramers-ion calculations as one which can give some of the possible configurations of

TABLE III. Table of configurations of the moments at different ionic sites, and the constant of proportionality $\lambda$ between the field at a site and the moment at that site. The sites are numbered as in Fig. 7. The moments at each site are equal in magnitude: the sign of the moment for ions 1–8 is as given in the table; the sign of moment for ions 9–16 is either as given in the table, in which case the constant of proportionality is denoted by $\lambda_+$, or the opposite to that in the table, in which case the constant of proportionality is denoted by $\lambda_-$. Values of $\lambda$ are to be multiplied by $10^{21}$ and the result is in $\text{cm}^{-3}$. The demagnetizing field correction is $6.908 \times 10^{21}$ $\text{cm}^{-3}$. The "corrected" value of $\lambda$ for the ferromagnetic configuration is $+13.850 \times 10^{21}$ $\text{cm}^{-3}$.

| 1 | 2 | 3 | 4 | 5 | 6 | 7 | 8 | | | |
|---|---|---|---|---|---|---|---|---|---|---|
| 9 | 10 | 11 | 12 | 13 | 14 | 15 | 16 | $\lambda_+$ | | $\lambda_-$ |
| + | + | + | + | + | + | + | + | + 6.942 | | +12.907 |
| + | − | + | − | + | − | + | − | +13.535 | | +13.217 |
| + | + | − | − | + | + | − | − | | | |
| + | + | + | + | − | − | − | − | | −10.696 | |
| + | − | − | + | + | − | − | + | +13.217 | | +13.535 |
| + | + | − | − | − | − | + | + | | | |
| + | − | + | − | − | + | − | + | | − 9.812 | |
| + | − | − | + | − | + | + | − | | | |

non-Kramers systems, but which does not give all the possible configurations. If, by this method, we find a configuration with low energy, in which all the ions have moments close to the maximum possible, then we may conjecture that there is probably no other configuration of lower energy. The reason is that the energy is $-\sum \mu_i H_i$; the $\mu_i$ are all almost as large as they can be, and $H_i$ depend linearly on the $\mu_i$ and therefore cannot be much increased without increasing the $\mu_i$, hence there is little freedom to find a configuration of significantly lower energy. In terbium ethylsulphate, the spontaneous magnetization appears to be about 0.8 of the maximum possible.

## V. CONCLUSIONS

We have demonstrated that terbium ethylsulphate, at temperatures below the transition at 240 mK, is ferromagnetic with the magnetization parallel to the hexagonal axis, in long thin domains also parallel to this axis. These observations are in accordance with molecular field calculations.

The ground state of the $Tb^{+++}$ ion consists of two singlets separated by an energy $\Delta$ whose value is of the order of 1 K. This is the only unknown parameter which describes the ground state, and we have attempted to measure its value. Unfortunately, our measurements do not lead to consistent results, indicating that there is a problem yet to be resolved.

The theory of the properties of this ground state has been reviewed by Abragam and Bleaney.[19] The theory gives a relation between $g-18$ and $\Delta$; however, not all the parameters which enter into this calculation are known, and it is admitted that the uncertainties in the calculated value of $\Delta$ are almost as large as $\Delta$ itself. As a result, there is one published value of $\Delta$ for the dilute salt, none for the concentrated salt, and no reliable means of calculating what $\Delta$ ought to be.

The other terms in the spin Hamiltonian have been measured. The value of $g$, $17.82 \pm 0.05$, though not very precise, is larger than the value 17.72 for the dilute salt, and, if the theory is to be believed, $\Delta$ should be smaller than the value of 0.56 K found for the dilute salt. We have attempted to determine $\Delta$ by fitting calculated magnetization curves to our observations above the transition temperature; the results are given in Table I. First of all, runs 1 and 2 show consistently larger values of $\Delta$ than do runs 3, 4, and 5. However, runs 1 and 2 were made at quite low temperatures, very close to the transition temperature, and may therefore be suspect on this account. The only other adjustible constant in the calculated magnetization curve is the value of the interaction field. This is composed of two parts added together, a Lorentz-type term and a demagnetization term. We have calculated the Lorentz term assuming only magnetic dipole interaction and no exchange. If this assumption is wrong, its effects could easily be interpreted as an incorrect demagnetizing factor. However, there is abundant evidence from all sorts of sources that there is no exchange coupling between rare-earth ions in the ethylsulphates.

Now, as is seen from Fig. 2, the errors in the fit are systematic. This is usually an indication that the wrong curve is being fitted, but it is not easy to see what could be wrong with the fitted curve as long as the spin Hamiltonian is accepted. If we allow the demagnetizing factor to be adjustable, we get better fits with a larger demagnetizing factor, leading to a smaller value of $\Delta$; the best fits are obtained with an unphysically large demagnetizing factor.

Fitting to measurements below the transition, however, favors a large value of $\Delta$ ($\cong 1.3$ K) and a small demagnetizing factor. However, the model used can easily be criticized as being too simple to be a good description of the actual magnetic behavior. Although there are no published measurements of $\Delta$ for the concentrated salt, recent unpublished measurements of the specific heat[5] indicate that $\Delta$ cannot be as large as the value 1.3 K indicated by these measurements in the ferromagnetic phase.

We therefore conclude that the most reliable value of $\Delta$ that can be obtained from our measurements is that given by the fitting of a calculated curve in the paramagnetic phase to runs 3, 4, and 5; permitting $\Delta$ to be the only adjustable parameter, and giving the other parameters their independently determined values. This value is $\Delta = 0.9 \pm 0.2$ K.

## ACKNOWLEDGMENT

We are indebted to the National Research Council of Canada for partial financial support. Financial support from the Jenny and Antti Wihuri Foundation is gratefully acknowledged.

## APPENDIX

In order to describe the polarization state of the light beam, let us take a right-handed set of rectangular axes ($x$, $y$, $z$) where the $+z$ direction is the direction of propagation of the light. The $x$ direction may be arbitrarily chosen, and it serves as the zero of azimuth. Positive angles are measured from the $+x$ axis towards the direction of the $+y$ axis. Photons in the beam have two spin states, let us take as a basis in the 2-dimensional spin

space $\binom{1}{0}$, which corresponds to the spin of the photon being in the $+z$ direction, and $\binom{0}{1}$, which corresponds to the spin of the photon being in the $-z$ direction. In the former case, the $\vec{E}$ vector in the $x$-$y$ plane rotates in a positive direction, and in the latter case in a negative direction. Further, the phases are chosen so that, in both cases, the $\vec{E}$ vector lies along the $y$ axis at time $t=0$. (These states correspond to right- and left-handed circularly polarized light; we shall, however, refrain from using these terms, since there are in current use two opposite conventions which define them.)

Elliptically polarized light, in which the tip of the $\vec{E}$ vector moves in a positive direction around an ellipse as shown in Fig. 8, can be represented either by the state vector

$$\frac{i}{\sqrt{2}}\begin{bmatrix}(\cos\beta+\sin\beta)e^{-i\alpha}\\ -(\cos\beta-\sin\beta)e^{i\alpha}\end{bmatrix}$$

or by the density matrix

$$\tfrac{1}{2}\begin{bmatrix}1+\sin2\beta & -\cos2\beta e^{-2i\alpha}\\ -\cos2\beta e^{2i\alpha} & 1-\sin2\beta\end{bmatrix}.$$

In particular, light which is plane polarized with $\vec{E}$ making an angle $\theta$ with the $x$ axis is represented by the density matrix

$$P=\tfrac{1}{2}\begin{bmatrix}1 & -e^{-2i\theta}\\ -e^{2i\theta} & 1\end{bmatrix}.$$

The mica plate has two axes at right angles. When the $\vec{E}$ vector lies along one of these, the "fast" direction, light travels faster than when it lies along the perpendicular "slow" direction. The mica plate introduces a phase difference $\delta$ between the components of light polarized in these two directions. If the "fast" axis makes an angle $+\phi$ with the $x$ axis, then the mica plate can be represented by a unitary matrix

$$U=\begin{bmatrix}\cos\tfrac{1}{2}\delta & ie^{-2i\phi}\sin\tfrac{1}{2}\delta\\ ie^{2i\phi}\sin\tfrac{1}{2}\delta & \cos\tfrac{1}{2}\delta\end{bmatrix}.$$

Suppose the polarization state of the incident light is represented by a density matrix

$$\rho=\begin{bmatrix}a+b & c-id\\ c+id & a-b\end{bmatrix}.$$

Then, after this light has passed through the mica plate, its density matrix is $U\rho U^*$, and after it has then passed through the analysing polaroid, its intensity is $\mathrm{Tr}(PU\rho U^*)$, which is

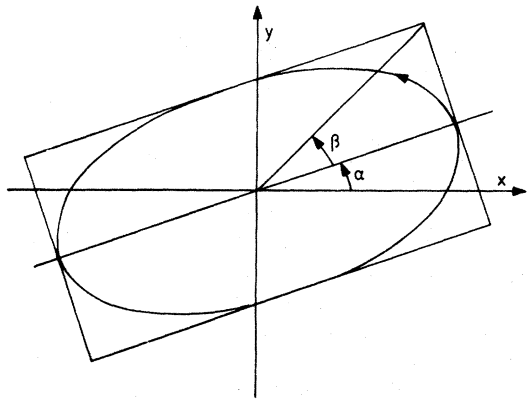


FIG. 8. Definition of parameters for describing the polarization of light.

$$a+b\sin\delta\sin(2\phi-2\theta)$$
$$-c[\cos^2\tfrac{1}{2}\delta\cos2\theta+\sin^2\tfrac{1}{2}\delta\cos(4\phi-2\theta)]$$
$$-d[\cos^2\tfrac{1}{2}\delta\sin2\theta+\sin^2\tfrac{1}{2}\delta\sin(4\phi-2\theta)]\,.$$

In order to determine $a$, $b$, $c$, and $d$, four readings are required with different values of $\theta$ and $\phi$. We decided, for reasons of experimental convenience, to choose as possible values of $\theta$ and $\phi$, $\theta=\pm\Theta/2$ and $\phi=\pm\Theta/2$. Substituting these values into the intensity formula, we find that $a$, $b$, $c$, and $d$ are the unknowns in four linear simultaneous equations, whose coefficients are functions of $\Theta$ and $\delta$. These equations are well conditioned provided that $\sin\Theta$, $\sin\Theta\sin2\Theta$, and $2\sin^2\tfrac{1}{2}\delta\sin\Theta\sin2\Theta$ are all large. We chose, as our criterion that $\sin\theta\sin2\theta$ should be a maximum. This occurs when $\Theta=54.8°$, thus $\theta,\phi=\pm27.4°$. Expressing $\rho$ as a linear combination of the unit matrix and the density matrix for elliptically polarized light, we find

$$\tan2\alpha=d/c,\quad \tan2\beta=b/(c^2+d^2)^{1/2},$$

and the intensity fraction of unpolarized light is given by

$$(b^2+c^2+d^2)/a^2\,.$$

In our experiment, we constructed the polarimeter as closely as possible to the design, and calibrated it (i.e., measured the constants in the relation between $a$, $b$, $c$, and $d$, on the one hand, and the four measured intensities on the other hand) by observing the readings with light of known polarization.

Suppose now we have a mixture of light of different plane polarizations, and suppose that the light for which the rotation lies between $\theta$ and $\theta+\delta\theta$ has an intensity $f(\theta)\delta\theta$. Then the density matrix of the mixture is

$$\int \tfrac{1}{2}\begin{bmatrix} 1 & -e^{-2i\theta} \\ -e^{2i\theta} & 1 \end{bmatrix} f(\theta)d\theta \Big/ \int f(\theta)d\theta$$
$$= \tfrac{1}{2}\begin{bmatrix} 1 & -\langle f(\theta)\cos 2\theta\rangle + i\langle f(\theta)\sin 2\theta\rangle \\ -\langle f(\theta)\cos 2\theta\rangle - i\langle f(\theta)\sin 2\theta\rangle & 1 \end{bmatrix}.$$

If now, $f(\theta)$ is a symmetric function, whose maximum we may take to be at $\theta = 0$ without any loss of generality, then $\langle f(0)\sin 2\theta\rangle = 0$, and the density matrix can be written

$$\tfrac{1}{2}(1 - \langle f(\theta)\cos 2\theta\rangle)\begin{bmatrix} 1 & 0 \\ 0 & 1 \end{bmatrix} + \tfrac{1}{2}\langle f(\theta)\cos 2\theta\rangle \begin{bmatrix} 1 & -1 \\ -1 & 1 \end{bmatrix},$$

which represents a mixture of unpolarized light of fractional intensity $1 - \langle f(\theta)\cos 2\theta\rangle$ and light, polarized in the plane $\theta = 0$, of fractional intensity $\langle f(\theta)\cos 2\theta\rangle$. We see therefore that a spread in the rotation of the plane of polarization of the emergent light introduces an unpolarized component, but does not affect the measurement of the central value of the rotation, provided that the spread is distributed symmetrically about its maximum. If the spread $f(\theta)$ is not symmetrical, then the polarizer will measure the intensity-weighted average rotation, provided the spread is so small that we can approximate $\cos 2\theta$ by 1 and $\sin 2\theta$ by $2\theta$ over the range of values for which $f(\theta)$ is not negligible. In this case, the intensity fraction of unpolarized light is zero. In all cases, the effect is to produce a mixture of unpolarized light and plane-polarized light (because the diagonal elements of the density matrix are equal). If the spread is Gaussian, $f(\theta) = e^{-\theta^2/2\sigma^2}/\sigma\sqrt{2\pi}$, then the intensity fraction of unpolarized light is $1 - e^{-2\sigma^2}$.

*On leave of absence from the University of Toronto, Toronto, Ontario, Canada.

[1]G. T. Trammell, J. Appl. Phys. 31, 362S (1960); Phys. Rev. 131, 932 (1963).
[2]For example, see B. Bleaney, Proc. R. Soc. A 276, 19 (1963); Y. L. Wang and B. R. Cooper, Phys. Rev. 172, 539 (1968); Phys. Rev. 185, 696 (1969).
[3]R. J. Anderson, I. Baker, and R. Birgeneau, J. Phys. C 4, 1618 (1971).
[4]See, for example, A. H. Cooke, D. T. Edmonds, C. P. Finn, and W. P. Wolf, Proc. R. Soc. A 306, 313 (1968).
[5]M. T. Hirvonen, T. E. Katila, K. J. Riski, M. A. Teplov, B. Z. Malkin, N. E. Phillips, and Marilyn Wun Phys. Rev. B (to be published).
[6]See, for example, J. F. Dillon, Jr., H. Kamimura, and J. P. Remeika, J. Appl. Phys. 34, 1240 (1963).
[7]Obtained from Kemira Oy, Malminkatu 30, Helsinki 10.
[8]G. J. Ehnholm, T. E. Katila, O. V. Lounasmaa, and P. Reivari, Cryogenics 8, 136 (1968); G. M. Kalvius, T. E. Katila, and O. V. Lounasmaa, *Mössbauer Effect Methodology*, edited by I. J. Gruverman (Plenum, New York, 1970), Vol. 5, p. 231.
[9]Type "Airam" HgL N4 125 W.
[10]Type "Stycast" 2850 GT obtained from Emerson and Cuming Europe N. V., Nijverheidsstraat 24, Oevel, Belgium.
[11]No. 9524A, supplied by Nuclear Enterprises G. B. Ltd., Sighthill, Edinburgh 11, Scotland.
[12]S. R. King and C. D. Jeffries, Bull. Am. Phys. Soc. 13, 434 (1968).
[13]J. M. Baker and B. Bleaney, Proc. R. Soc. A 245, 156 (1958).
[14]J. A. A. Ketelaar, Physica (Utr.) 4, 619 (1937).
[15]J. M. Luttinger and L. Tisza, Phys. Rev. 70, 954 (1946).
[16]A. Gavignet-Tillard, J. Hamman, and L. de Seze, J. Phys. (Paris) 34, 27 (1973).
[17]E. Lagendijk, H. W. T. Blöte, and W. J. Huiskamp, Physica (Utr.) 61, 230 (1972).
[18]R. Bidaux, A. Gavignet-Tillard, and J. Hamman, J. Phys. (Paris) 34, 19 (1973).
[19]A. Abragam and B. Bleaney, *Electron Paramagnetic Resonance of Transition Ions* (Oxford U. P., London, 1970), pp. 317 and 378.